SUPPLEMENTAL MATERIALS

CD47 activation by thrombospondin-1 in lymphatic endothelial cells suppresses lymphangiogenesis and promotes atherosclerosis

Bhupesh Singla[1*], Ravi Varma Aithbathula[1], Naveed Pervaiz[1], Ishita Kathuria[1], Mallory Swanson[1], Frederick Adams Ekuban[1], WonMo Ahn[2], Frank Park[1], Maxwell Gyamfi[1], Mary Cherian-Shaw[2], Udai P Singh[1] and Santosh Kumar[1]

[1]Department of Pharmaceutical Sciences, College of Pharmacy, The University of Tennessee Health Science Center, USA and [2]Vascular Biology Center, Medical College of Georgia, Augusta University, USA.

[*]Corresponding Author:
Bhupesh Singla, Ph.D.
Assistant Professor
881 Madison Ave, Room 446
Department of Pharmaceutical Sciences, College of Pharmacy
The University of Tennessee Health Science Center,
Memphis, TN 38163, USA
Phone: + 1 901-448-4135, Fax: + 1 901-448-3446
e-mail: bsingla@uthsc.edu

Supplemental Materials and Methods

Cell proliferation assay

LEC proliferation was measured using Cell Proliferation Reagent WST-1 (Roche Diagnostics GmbH, Mannheim, Germany, 5015944001). Briefly, 10,000 cells/well were seeded in a 96-well plate. Next day, cells were pretreated with vehicle (PBS) or human recombinant TSP1 at indicated concentrations (Sigma-Aldrich, ECM002) in basal medium MV 2 media containing 0.5% FBS for 4 h and stimulated with human recombinant VEGF-C (100 ng/mL, Peprotech, Rocky Hill, NJ, 100-20CD). After given incubation times, 10 µL WST-1 reagent was added to each well, and the plate was incubated at 37°C for an additional 3 h. Absorbance at 450 nm was measured using a Cytation 5 Reader (Biotek Instruments Inc., Winooski, VT). Absorbance at 690 nm was taken as a reference.

For determination of Ki67-positive cells, LEC-plated on coverslips were pretreated with vehicle or TSP1 (22 nM) for 4 h and stimulated with VEGF-C (100 ng/mL) for 24 h. Next, cells were fixed, permeabilized, blocked, and incubated with Ki67 primary antibody (Cell Signaling Technology, 9129, 1:100) overnight at 4°C. Cells on coverslips were then incubated with fluorescently-labeled secondary antibodies (Life Technologies Corporation) and mounted with DAPI containing Fluoromount-G. Images were captured using a Zeiss 710 inverted confocal microscope, and Ki67-positive cells counted using the NIH Image J software.

Cell Migration Assay

LEC migration was investigated using Culture-Insert 2 Well 24 (ibidi USA, Inc., Fitchburg, WI, USA) as described previously [1]. Cells were pretreated with vehicle or TSP1 (11 nM & 22 nM) for 4 h and stimulated with VEGF-C (100 ng/mL) for 24 h at 37 °C. Images of wounds at 0 h were captured using an inverted EVOS™ FL Imaging System (Thermo Fisher Scientific). After 24 h of VEGF-C stimulation, cell layers were washed, fixed, permeabilized, stained with Alexa Fluor 488-phalloidin, and images were taken. Area of wounds at 0 h and 24 h were determined using the Image-Pro Plus software (Media Cybemetics, Bethesda, MD, USA). The percentage of wound closure was calculated.

In separate experiments, Boyden chamber assay was performed to investigate LEC migration in response to TSP1 treatment. Briefly, vehicle- or TSP1-pretreated LEC (4 h) were added to upper chambers of transwell inserts (20000 cells/well, 8 µm pore membranes, Corning, NY, USA) in VEGF-C containing media in the presence or absence of TSP1, and the number of cells migrated to lower side of the membrane was quantified (16 h). Images of at least 5 random microscopic fields were captured.

Lymphangiogenesis Assay

A Matrigel tube formation assay was done to investigate *in vitro* lymphangiogenesis [2]. Briefly, vehicle- or TSP1-pretreated LEC (20 000 cells/well) in basal medium MV 2 (0.5% FBS) containing VEGF-C with or without TSP1 were seeded onto solidified Matrigels and incubated for 6 h at 37°C in a humidified incubator with 5% CO_2. Matrigels were stained with Alexa Fluor 488-phalloidin, and images were recorded using an inverted EVOS™ FL Imaging System (Thermo Fisher Scientific). The tube length and number of branching points were measured using the NIH ImageJ software.

To investigate *in vivo* lymphangiogenesis, eight- to ten-week-old wild-type mice were injected subcutaneously (*s.c.*) with 400 µL of growth factor-reduced Matrigel premixed with

murine VEGF-C (100 ng/mL), VEGF-C + TSP1 (22 nM) + IgG control antibody (100 µg/mL, BioXcell, Lebanon, NH, BE0083), or VEGF-C + TSP1 + CD47 blocking antibody (100 µg/mL, BioXcell, BE0283). Mice were euthanized by isoflurane inhalation and cervical dislocation after 10 days of Matrigel implantation. Matrigel plugs were harvested and fixed in 10% neutral buffered formalin, and LYVE-1 immunostaining was performed on paraffin sections.

Cell Cycle Analysis

Cells were pretreated with vehicle or TSP1 (22 nM) for 4 h and stimulated with VEGF-C (100 ng/mL). After 24 h of incubation, cells were washed, fixed and stained with FxCycle™ PI/RNase Staining Solution for 30 min in dark at room temperature. The samples were immediately analyzed using a NovoCyte Flow Cytometer (Agilent, Santa Clara, CA).

Quantitative real-time PCR

Total cellular RNA from LEC was extracted using the IBI Tri-Isolate RNA Pure Kit (IBI Scientific, Dubuque, IA, USA) according to the manufacturer's protocol. High-Capacity cDNA Reverse Transcription Kit (Applied Biosystems, Carlsbad, CA, 4368814) was utilized to reverse transcribe RNA (500 - 700 ng) into complementary DNA. Quantitative real-time PCR was performed in a QuantStudio 3 Real-Time PCR System (Applied Biosystems) with Fast SYBR™ Green Master Mix (Applied Biosystems, 4385612) using gene-specific primers listed in **Table S2**. Relative gene expression was calculated with the $2^{-\Delta\Delta Ct}$ method using GAPDH as an internal control.

Reactive oxygen species generation

2′,7′-Dichlorofluorescin diacetate (Sigma-Aldrich, D6883) was used to determine intracellular reactive oxygen species (ROS) production. Briefly, LEC-seeded in a 12-well plate were treated with vehicle or TSP1 (11 nM) for 60 min. Cells were then washed, incubated with serum-free media containing H2DCFDA (5 µM) for 30 min at 37°C and analyzed for fluorescence (Ex: 492 nm, Em: 525 nm) using a NovoCyte Flow Cytometer. Mean fluorescence intensity was used to compare ROS generation between groups.

Intracellular NO analysis

Cells plated in a 96-well plate (20,000 cells/well) were pretreated with vehicle or TSP1 (22 nM) for 4 h and stimulated with VEGF-C for 1 h. After the incubation time, cells were washed and incubated with DAF-FM diacetate solution (5 µM) for 45 min at 37°C. Then, cells were washed, incubated with fresh basal media without serum for 30 min, and fluorescence measured using excitation/emission spectra 495/515 nm with a Cytation 5 Reader (Biotek). Cells without the addition of DAF-FM diacetate solution were used to calculate background fluorescence.

Cytokine levels in mouse plasma samples

Cytokine levels in mouse plasma samples were quantified using the LEGENDplex™ bead-based immunoassay (BioLegend, San Diego, CA, mouse inflammation panel) according to the manufacturer's instructions. Fluorescence intensities were measured using the BD FACSCalibur (BD Biosciences, San Jose, CA, USA) and analyzed using the LEGENDplex Data Analysis software (BioLegend). The cytokine levels are shown in pg/mL.

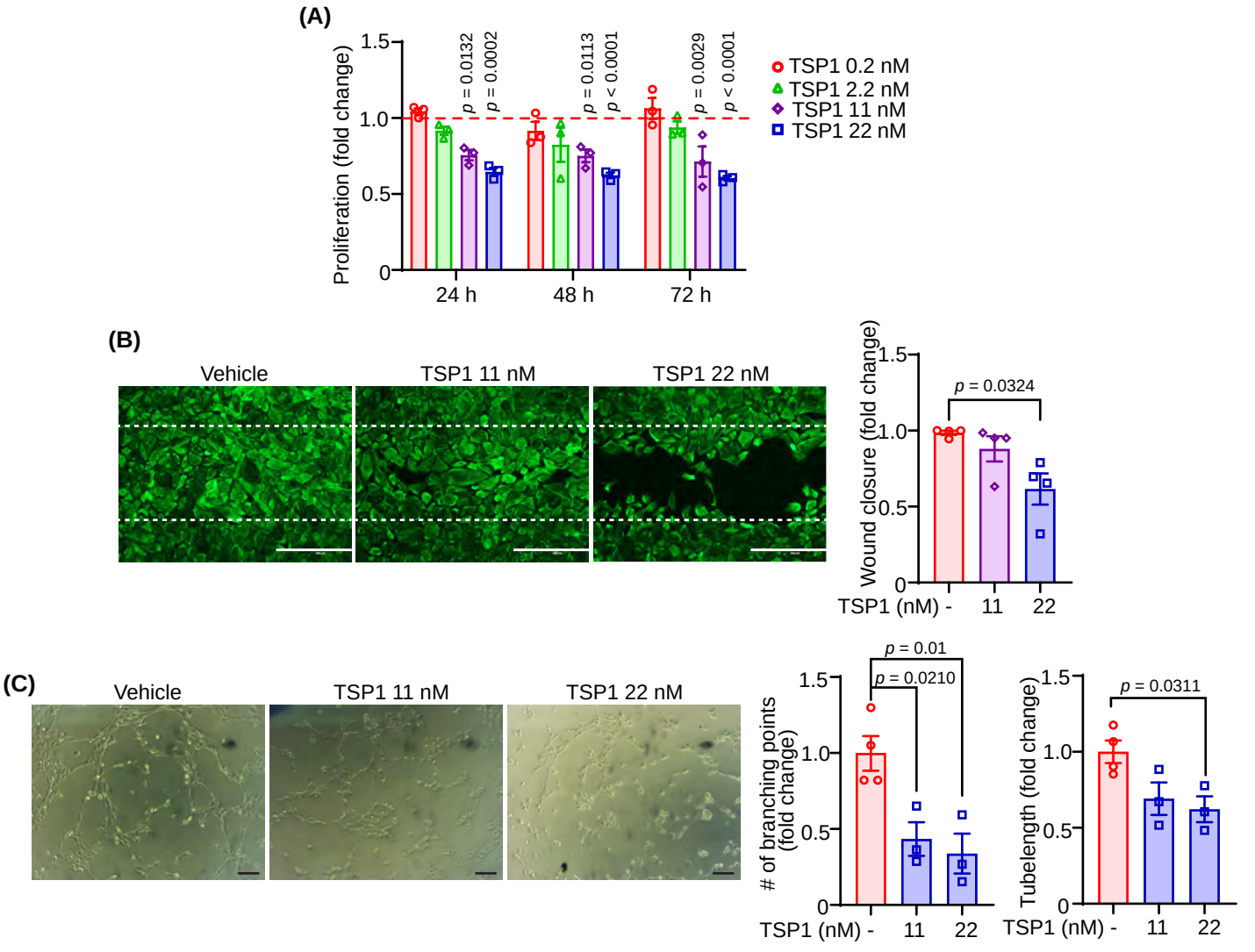

Figure S1. TSP1 inhibits lymphangiogenesis in vitro. **(A)** Human LEC were treated with vehicle or TSP1 (0.2 - 22 nM) for 4 h, stimulated with VEGF-C (100 ng/mL) for various time points, and cell proliferation investigated using WST-1 assay. The dotted red line indicates cell proliferation in control VEGF-C-stimulated cells. Data are representative of three independent experiments. The shown asterisks represent *P* values with respect to control. **(B)** LEC migration in response to TSP1 treatment after 24 h of VEGF-C stimulation ($n = 4$). Scale bar 400 µm. **(C)** Vehicle- or TSP1-treated LEC were seeded in wells of a Matrigel-coated plate in basal medium containing VEGF-C ± TSP1 and tube formation determined after 6 h. Representative images of tube formation are shown. Scale bar 50 µm. Images of random fields were captured, and tubelength and number of branching points quantified ($n = 3$ - 4). Statistical analyses were performed using two-way ANOVA with Tukey's multiple comparisons test **(A)**, Kruskal-Wallis test **(B)** and one-way ANOVA with Dunnett's multiple comparisons test **(C)**. Data represent mean ± SEM.

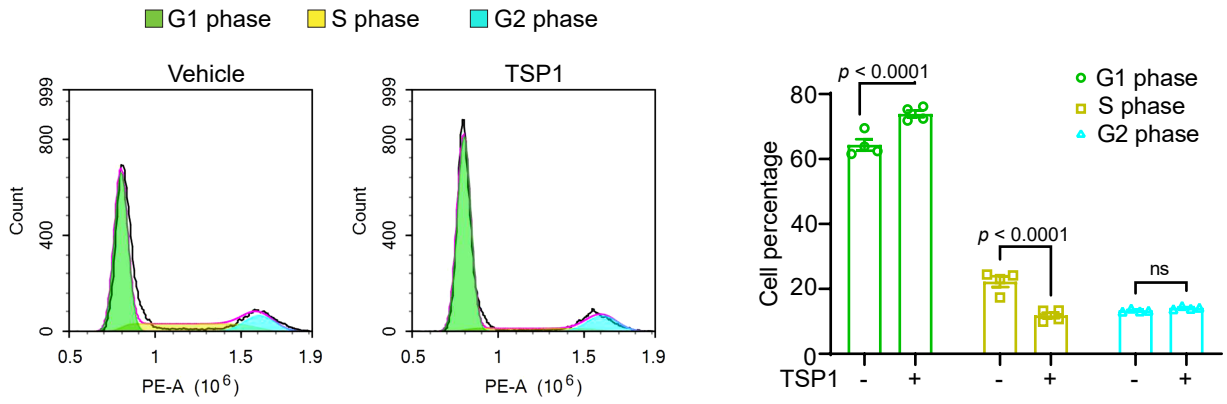

Figure S2. TSP1 induces cell cycle arrest in LEC. Human LEC were treated with vehicle or TSP1 (22 nM) for 4 h, stimulated with VEGF-C (100 ng/mL) for 24 h, and cell cycle analysis performed. Representative histograms indicating cells in G1, S and G2 phases are shown. Bar diagram shows cell percentage in various cell cycle phases (n = 4). Statistical analyses were performed using two-way ANOVA with Sidak's multiple comparisons test. Data represent mean ± SEM.

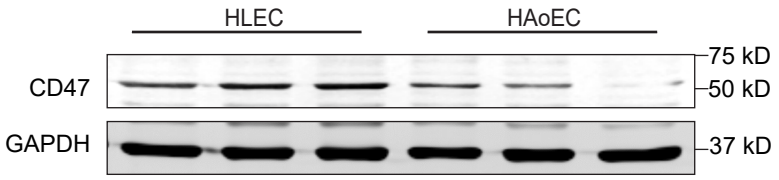

Figure S3. CD47 protein expression in human LEC and human aortic endothelial cells. Western blot images of CD47 (NBP2-31106) and GAPDH protein expression are shown ($n = 3$).

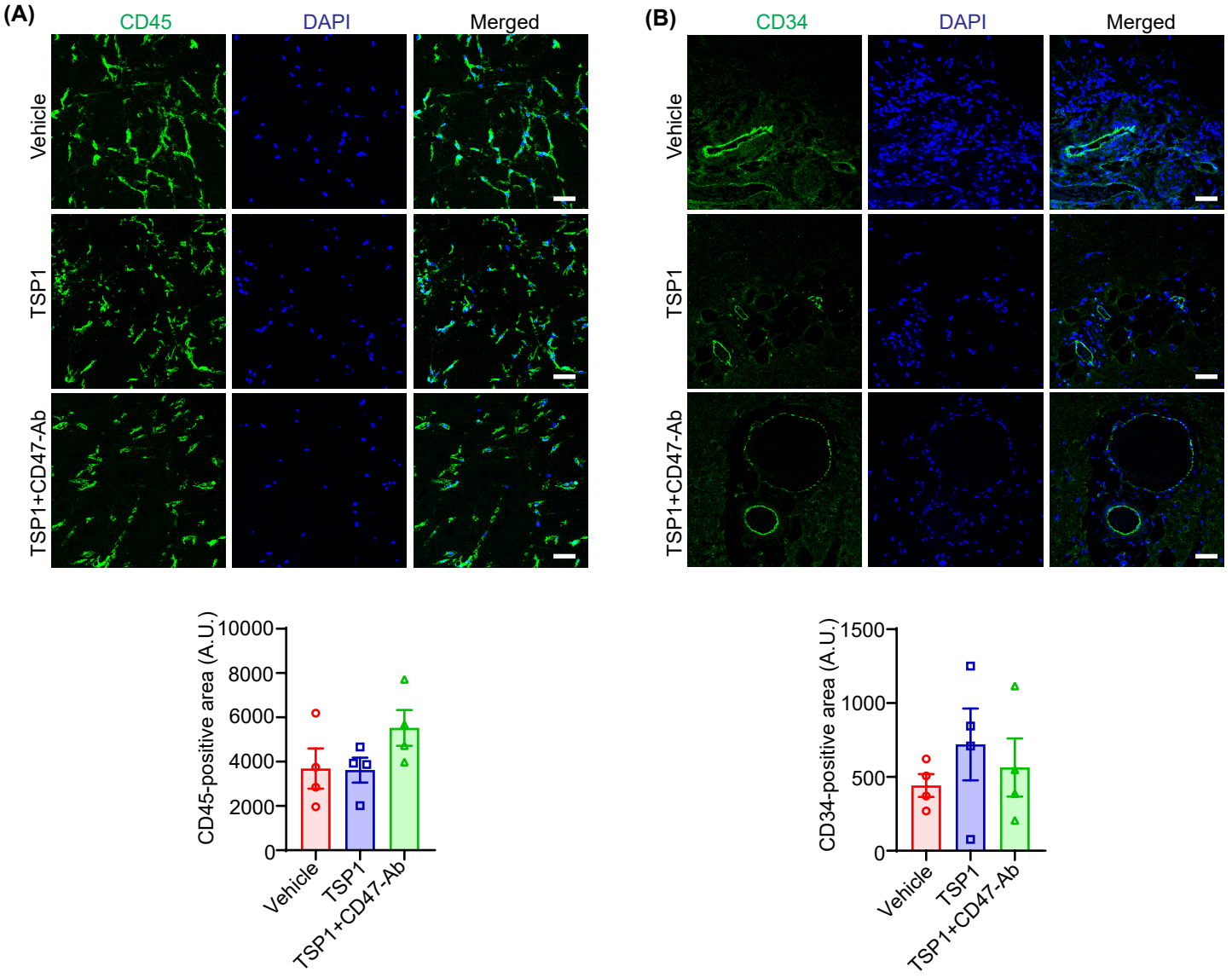

Figure S4. Immune cell infiltration and angiogenesis in Matrigel plugs. (A and B) Male wild-type mice were injected *s.c.* with Matrigel solutions premixed with either VEGF-C (vehicle), VEGF-C+TSP1 (TSP1) or VEGF-C+TSP1+CD47-blocking antibody (TSP1+CD47-Ab). Plugs were isolated after 10 days, sectioned and immunostained for CD45 and CD34 to determine immune cell infiltration and angiogenesis, respectively. Representative images of CD45 **(A)** and CD34 **(B)** immunostaining and quantification of CD45/CD34-positive area are shown (n = 4). Scale bar 50 µm. Statistical analyses were performed using one-way ANOVA with Tukey's multiple comparisons test. Data represent mean ± SEM.

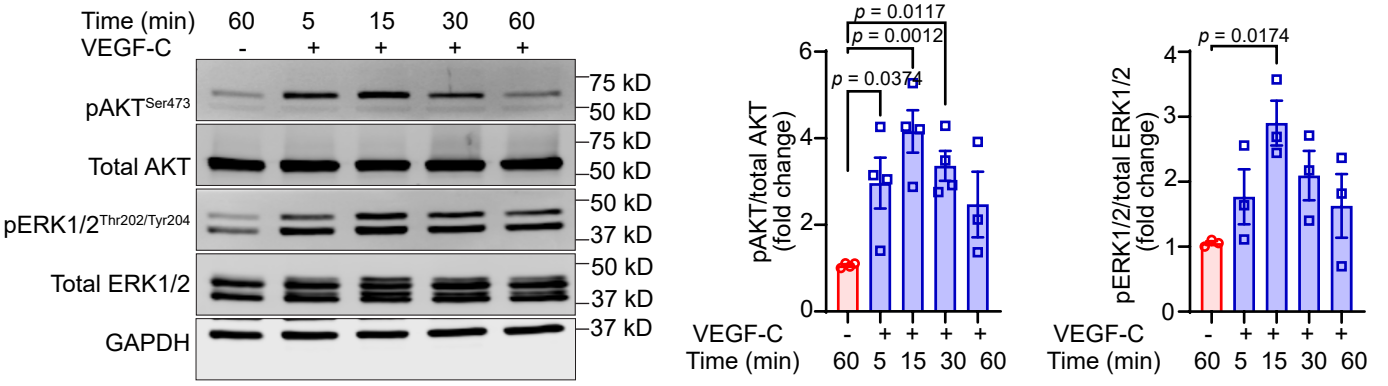

Figure S5. VEGF-C stimulates maximal activation of AKT and ERK1/2 after 15 min incubation. LEC were starved overnight in 0.5% FBS containing basal media MV2, treated with VEGF-C (100 ng/mL) for indicated time points, and cell lysates subjected to western blot analysis. Representative western blot images are shown. Bar diagrams represent mean protein levels expressed as a ratio of phospho to total proteins ($n = 3 - 4$). Statistical analyses were performed using one-way ANOVA with Dunnett's multiple comparisons test. Data represent mean ± SEM.

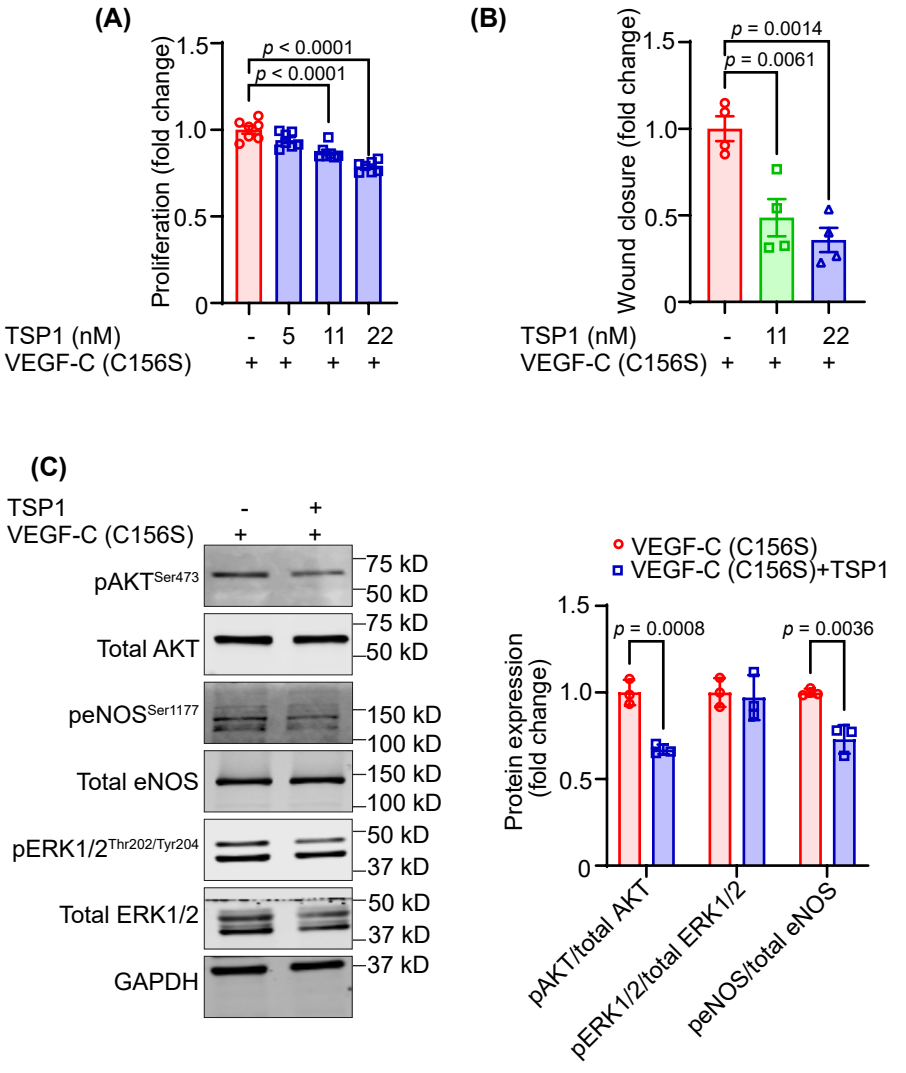

Figure S6. TSP1 suppresses VEGF-C (C156S)-stimulated lymphangiogenic signaling. **(A)** Human LEC were treated with vehicle or TSP1 (5, 11 and 22 nM) for 4 h, stimulated with VEGFR3-specific mutant VEGF-C (C156S) (100 ng/mL) for 48 h, and cell proliferation investigated using WST-1 assay ($n = 7$). **(B)** LEC migration in response to TSP1 treatment after 24 h of VEGF-C (C156S) stimulation ($n = 4$). **(C)** LEC were pretreated with TSP1 (22 nM, 16 h) in 0.5% FBS containing basal media MV2, stimulated with VEGF-C (C156S) (15 min), and cell lysates subjected to western blot analysis. Representative western blot images are shown. Bar diagrams represent mean protein levels expressed as a ratio of phospho to total proteins ($n = 3$). Statistical analyses were performed using one-way ANOVA with Dunnett's/Sidak's multiple comparisons test **(A and B)** and two-way ANOVA with Sidak's multiple comparisons test **(C)**. Data represent mean ± SEM. Data represent mean ± SEM.

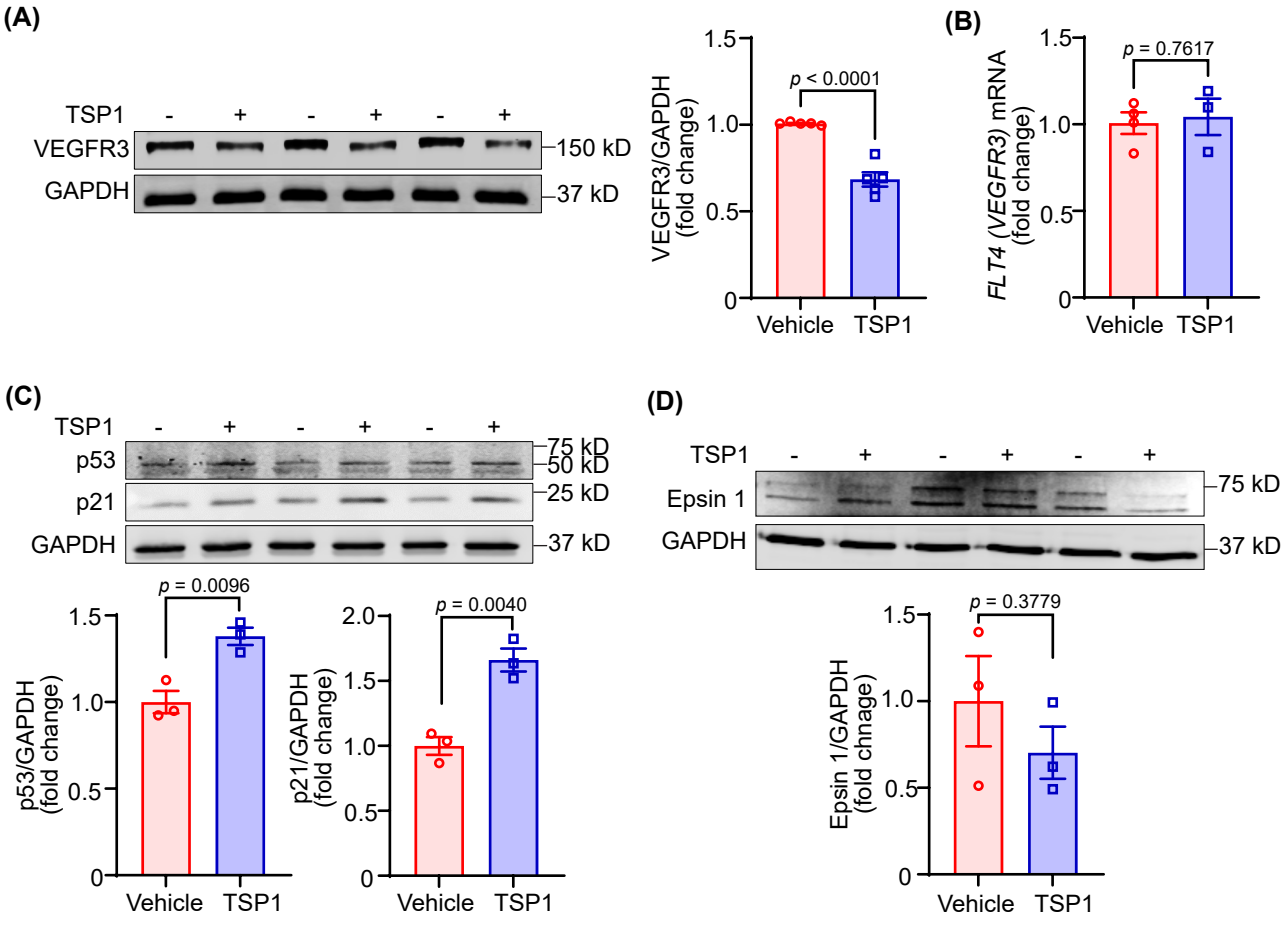

Figure S7. TSP1 treatment reduces VEGFR3 and induces p21 and p53 protein expression in LEC. LEC were treated with TSP1 (22 nM, 16 h) in 0.5% FBS containing basal media MV2 and cell lysates subjected to western blot analysis. **(A)** Representative western blot images and VEGFR3 expression normalized with GAPDH ($n = 5$). **(B)** Human LEC were treated with TSP1 (22 nM) for 24 h and qRT-PCR was performed to determine *FLT4* mRNA levels. **(C)** Representative western blot images and p53/p21 expression normalized with GAPDH ($n = 3$). **(D)** Representative western blot images and Epsin 1/GAPDH protein levels ($n = 3$). Statistical analyses were performed using a two-tailed unpaired *t*-test. Data represent mean ± SEM.

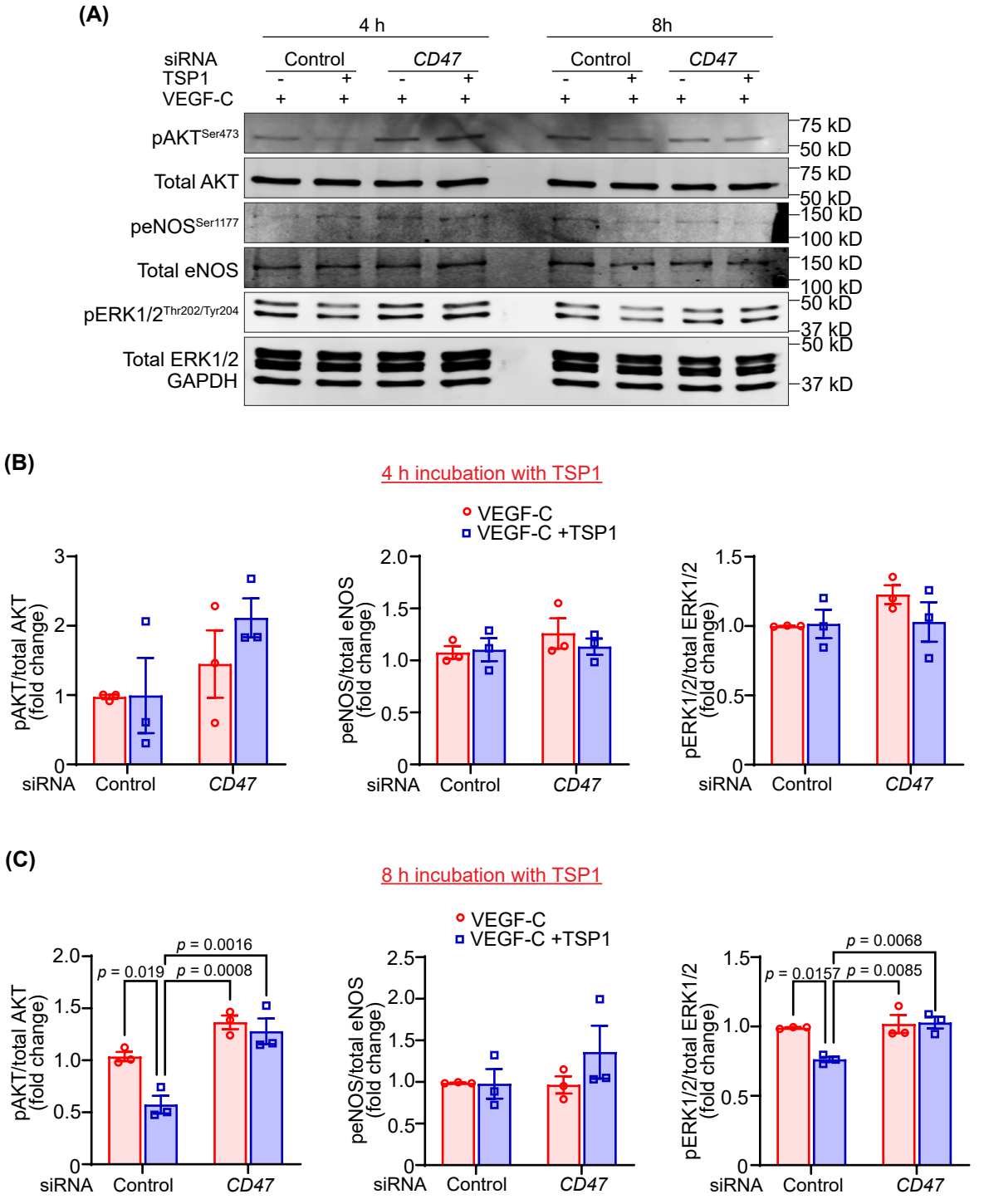

Figure S8. Effects of TSP1 treatment on VEGF-C-stimulated activation of AKT, eNOS and ERK1/2 at different time points. (A) Representative western blot images are shown. (B and C) Bar diagrams represent mean protein levels expressed as a ratio of phospho to total proteins (n = 3). Statistical analyses were performed using two-way ANOVA with Tukey's multiple comparisons test. Data represent mean ± SEM.

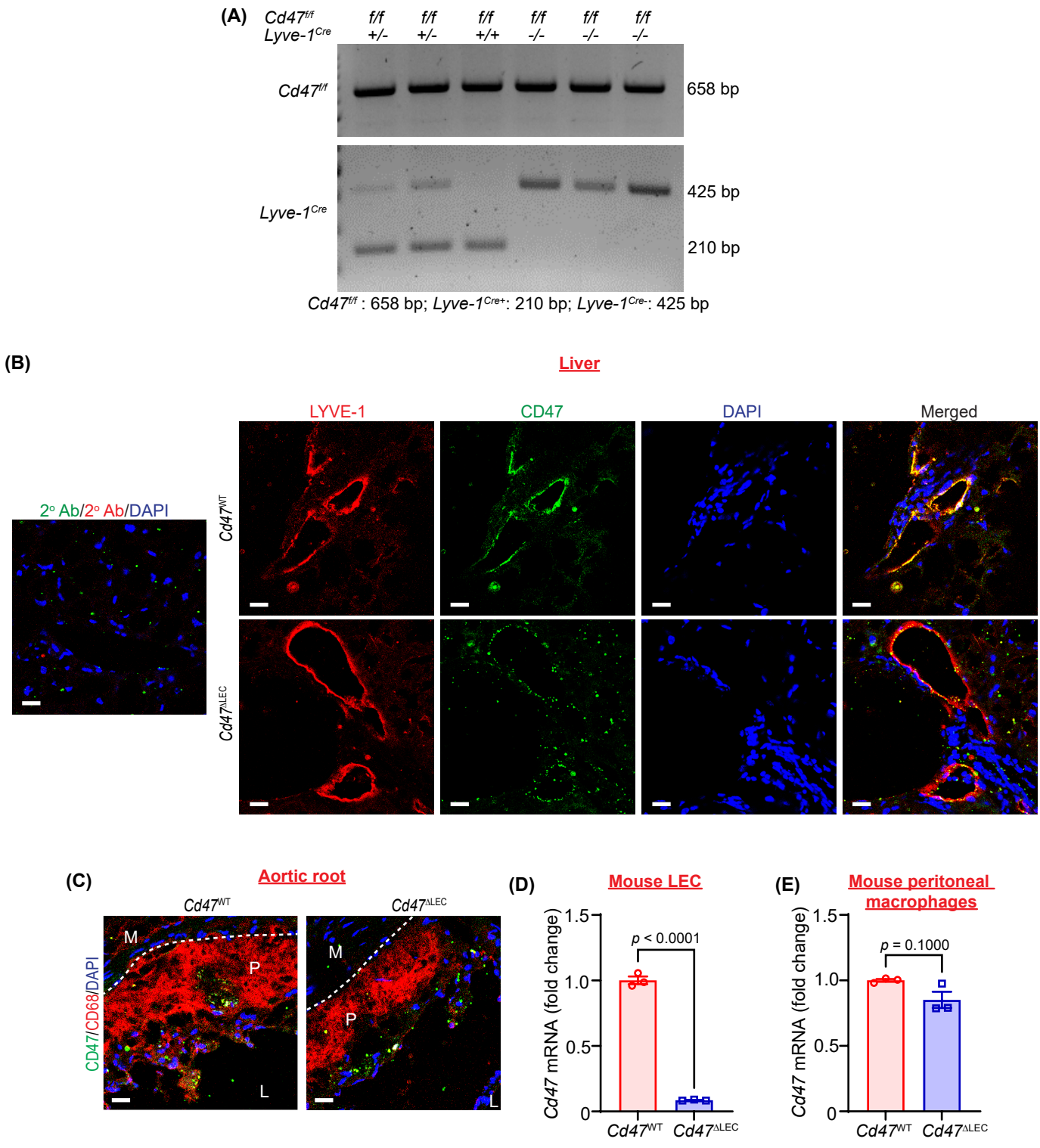

Figure S9. Confirmation of LEC-specific *Cd47* deletion. (A) Agarose gel showing representative genotyping experiments for *Cd47* flox and *Lyve-1* Cre. **(B)** Liver tissue cross-sections from male *Cd47*^{WT} and *Cd47*$^{\Delta LEC}$ mice were immunostained for LYVE-1 (red) and CD47 (green). Nuclei were counterstained with DAPI (blue). Scale bar 20 µm. **(C)** Immunostaining for CD47 (green) and CD68 (macrophage marker, red) using aortic root cross-sections of *Cd47*^{WT} and *Cd47*$^{\Delta LEC}$ mice. Scale bar 20 µm. **(D & E)** *Cd47* mRNA expression in lung LEC and thioglycollate-elicited peritoneal macrophages isolated from male mice. Statistical analyses were performed using two-tailed unpaired *t*-test **(D)** and Mann-Whitney test **(E)**. Data represent mean ± SEM. L: lumen, P: plaque and M: media.

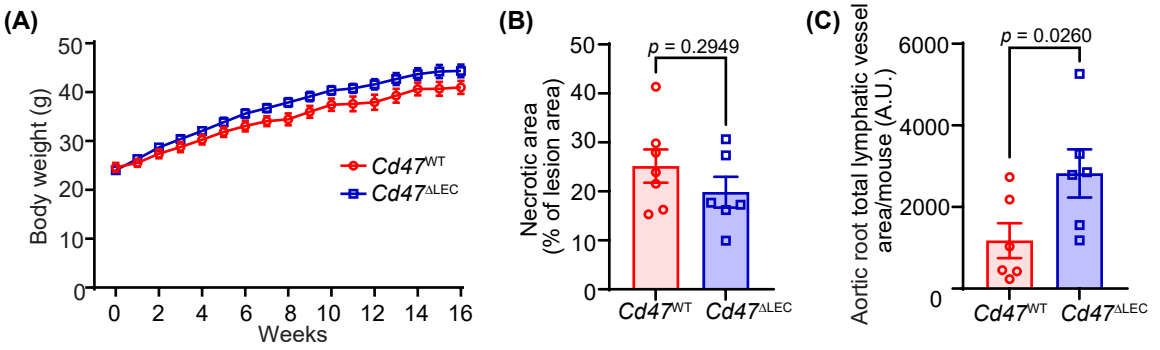

Figure S10. LEC-specific *Cd47* deletion does not alter weight gain. Male *Cd47*^{WT} and *Cd47*$^{\Delta LEC}$ mice were injected with AAV8-*PCSK9 i.p.*, fed a Western diet for 16 weeks. **(A)** Diagram shows body weight. **(B)** Aortic root necrotic area (n = 6-7). **(C)** Bar graph represents aortic root total LYVE-1-positive area/mouse (n = 6). Statistical analyses were performed using a multiple unpaired t-test **(A)**, two-tailed unpaired t-test **(B)** and two-tailed unpaired Mann-Whitney test **(C)**. Data represent mean ± SEM.

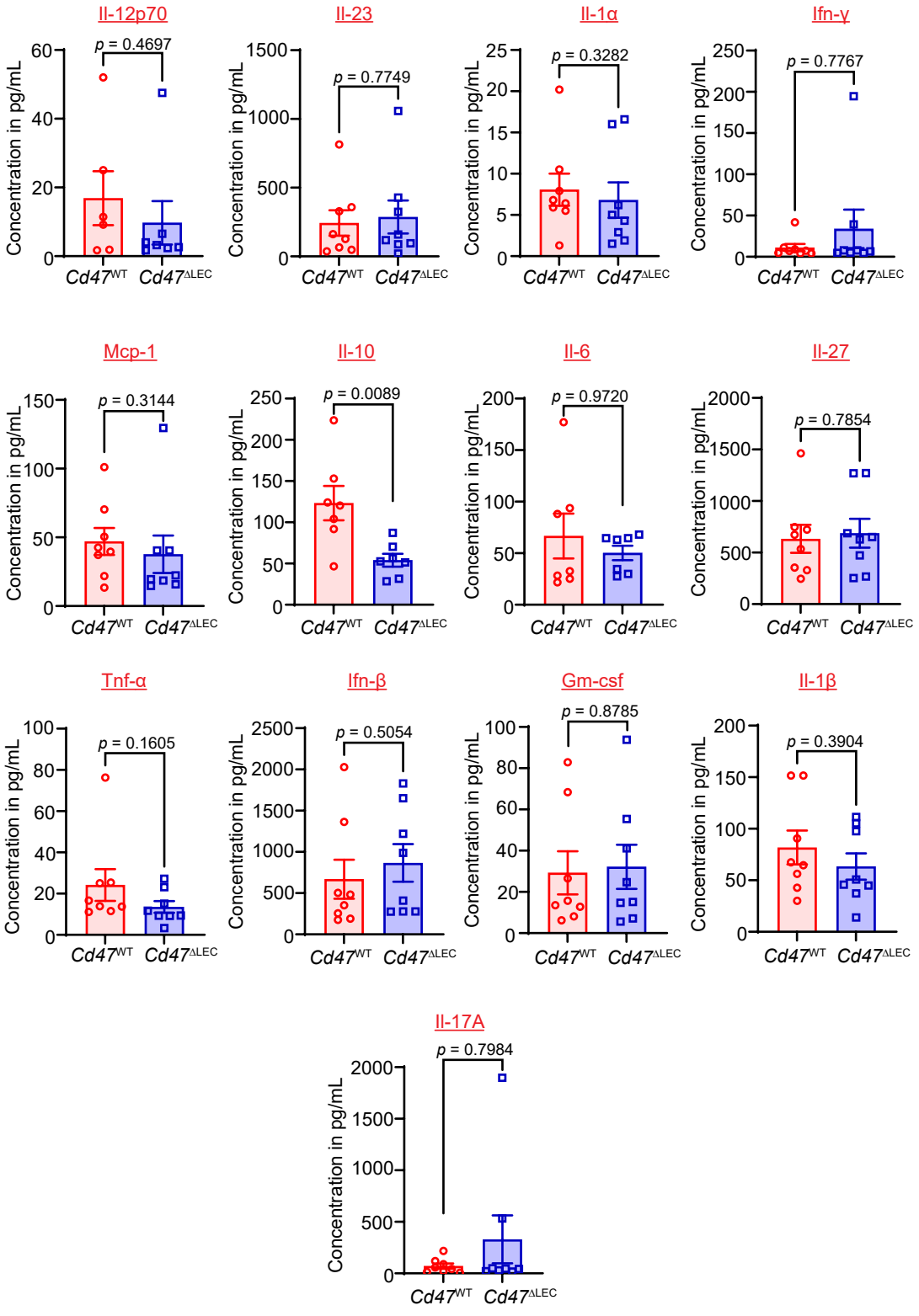

Figure S11. LEC-specific *Cd47* deletion does not affect plasma cytokine levels. Male *Cd47*^{WT} and *Cd47*$^{\Delta LEC}$ mice were injected with AAV8-*PCSK9 i.p.*, fed a Western diet for 16 weeks, and plasma cytokine levels analyzed using a LEGENDplex™ bead-based immunoassay (n = 6 - 8). Statistical analyses were performed using non-parametric Mann-Whitney test, except for Il-23, Il-1β, Il-10 and Il-27, which were compared using a two-tailed unpaired t-test. Data represent mean ± SEM.

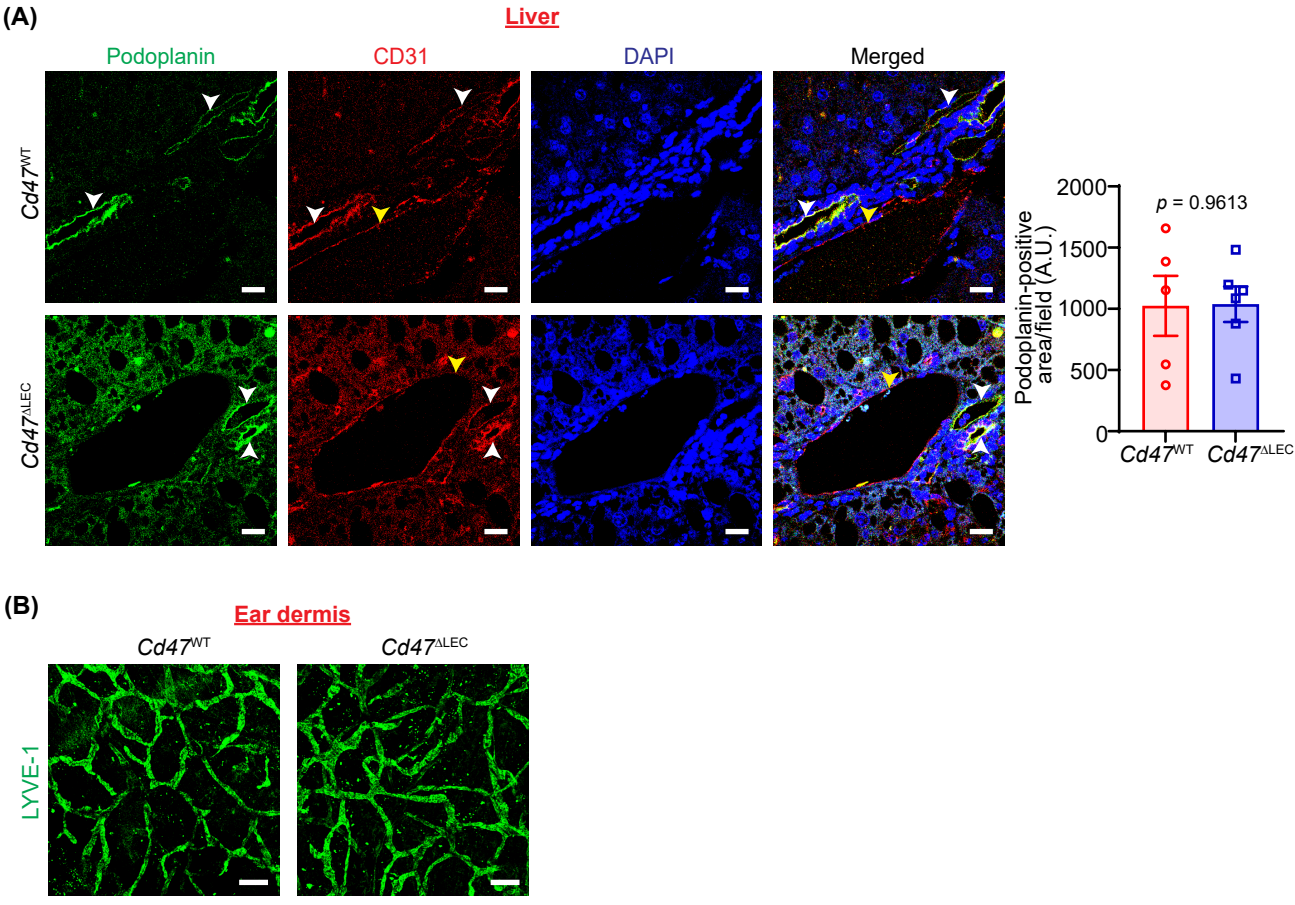

Figure S12. (A) Liver sections of male *Cd47*^{WT} and *Cd47*$^{\Delta LEC}$ mice were immunostained for podoplanin (LEC marker, green) and CD31 (endothelial cell marker). Nuclei were counterstained with DAPI (blue). Representative images are shown. Scale bar 20 µm. Bar graphs represent mean podoplanin-positive area/field (n = 5). White arrowheads: lymphatic vessels and yellow arrowheads: blood vessels. **(B)** Ear dermal sheets of male *Cd47*^{WT} and *Cd47*$^{\Delta LEC}$ mice were immunostained for LYVE-1 (green). Scale bar 200 µm. Statistical analyses were performed using a two-tailed unpaired *t*-test. Data represent mean ± SEM.

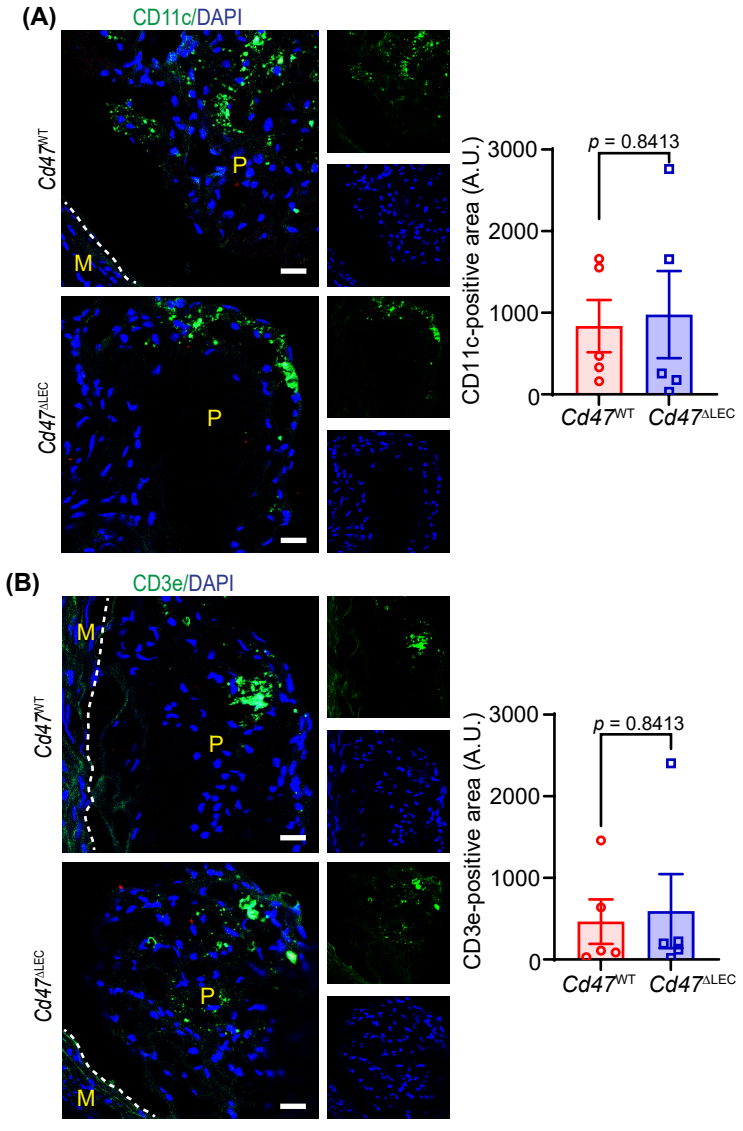

Figure S13. *Cd47*^{WT} and *Cd47*$^{\Delta LEC}$ mice have similar number of intraplaque dendritic cells and T-cells. Aortic root cross-sections from male AAV8-*PCSK9*-injected *Cd47*^{WT} and *Cd47*$^{\Delta LEC}$ mice (16 weeks Western diet) were immunostained for CD11c and CD3e. Nuclei were counterstained with DAPI (blue). Representative images of CD11c (green, **A**) and CD3e (green, **B**) are shown. Scale bar 20 µm. Bar graphs represent CD11c-positive area/mouse and CD3e-positive area/mouse. Images of CD11c- and CD3e-positive areas of entire aortic root section were captured. Statistical analyses were performed using a Mann-Whitney test. Data represent mean ± SEM.

Table S1: List of primers used for mice genotyping using conventional PCR.

Genotyping primer sequences	
***Apoe* knockout**	
ApoeF; 5'-GCC TAG CCG AGG GAG AGC CG-3' ApoeRW; 5'-TGT GAC TTG GGA GCT CTG CAG C-3' ApoeRM; 5'-GCC GCC CCG ACT GCA TCT-3'	Wild-type: 155 bp Heterozygous: 155 bp & 245 kb Mutant: 245 bp
***Lyve-1* Cre**	
10204; 5'-TGC CAC CTG AAG TCT CTC CT-3' 10205; 5'-TGA GCC ACA GAA GGG TTA GG-3' 10206; 5'-GAG GAT GGG GAC TGA AAC TG-3'	Mutant: 210 bp Heterozygous: 210 bp & 425 kb Wild-type: 425 bp
***Cd47* floxed**	
CSD-Cd47-F; 5'-TCTACACTAAACTCAGCTGGCCTGG-3' CSD-Cd47-ttR; 5'-CTGTCTCTGTGCTCTCTGGCTAAGG-3'	f/f: 658 bp f/+: 658 bp & 445 kb +/+: 445 bp

Table S2: List of primers used for mRNA quantitation using quantitative real-time PCR.

Gene name	Primer sequences
Human *CD36*	F 5'-CTT TGG CTT AAT GAG ACT GGG AC-3' R 5'-GCA ACA AAC ATC ACC ACA CCA-3'
Human *CD47*	F 5'-AGA AGG TGA AAC GAT CAT CGA GC-3' R 5'-CTC ATC CAT ACC ACC GGA TCT-3'
Human *FLT4*	F 5'- CTG GAC CGA GTT TGT GGA GG-3' R 5'- GTC ACA TAG AAG TAG ATG AGC CG-3'
Human *GAPDH*	F 5'- CATGTTCGTCATGGGTGTGAACCA-3' R 5'- AGTGATGGCATGGACTGTGGTCAT-3'
Mouse *Cd47*	F 5'- CAC GGC CTT CAA CAC TGA C-3' R 5'- ACA GGA GTA TAG CCA AAA TTG GG-3'
Mouse *Gapdh*	F 5'- AGG TCG GTG TGA ACG GAT TTG-3' R 5'- GGG GTC GTT GAT GGC AAC A-3'

Major Resources Table

Animals (*In vivo* study)

Species	Vendor/Source	Background strain	Sex	Persistent ID/URL
Mouse Wild-type	The Jackson Laboratory, stock # 000664	C57BL/6J	Male	https://www.jax.org/strain/000664
Mouse *Apoe*$^{-/-}$	The Jackson Laboratory, stock # 002052	C57BL/6J	Male	https://www.jax.org/strain/002052
Mouse *Lyve-1 Cre*$^{+}$	The Jackson Laboratory, stock # 012601	C57BL/6J	Female and Male	https://www.jax.org/strain/012601
Mouse *Cd47*$^{tm1a(KOMP)Mbp}$	Mouse Biology Program, University of California, Davis	C57BL/6	Female and Male	https://www.mmrrc.org/catalog/locus_detail.php?mgi_id=MGI:4455408

Antibodies

Target antigen	Vendor/ Source	Cat #	Working conc.	Persistent ID/URL
Total AKT	Cell Signaling Technology	2920S	1:1000	https://www.cellsignal.com/products/primary-antibodies/akt-pan-40d4-mouse-mab/2920?site-search-type=Products&N=4294956287&Ntt=2920s&fromPage=plp&_requestid=1356825
pAKT^{Ser473}	Cell Signaling Technology	4060S	1:1000	https://www.cellsignal.com/products/primary-antibodies/phospho-akt-ser473-d9e-xp-rabbit-mab/4060?site-search-type=Products&N=4294956287&Ntt=4060s&fromPage=plp&_requestid=1356896
peNOS^{Ser117}	Cell Signaling Technology	9571S	1:1000	https://www.cellsignal.com/products/primary-antibodies/phospho-enos-ser1177-antibody/9571?site-search-type=Products&N=4294956287&Ntt=9571s&fromPage=plp&_requestid=1356946
Total eNOS	Cell Signaling Technology	5880S	1:1000	https://www.cellsignal.com/products/primary-antibodies/enos-6h2-mouse-mab/5880?site-search-type=Products&N=4294956287&Ntt=5880s&fromPage=plp&_requestid=1357026
pERK1/2$^{Thr202/Tyr204}$	Cell Signaling Technology	9101S	1:1000	https://www.cellsignal.com/products/primary-antibodies/phospho-p44-42-mapk-erk1-2-thr202-tyr204-antibody/9101?site-search-type=Products&N=4294956287&Ntt=9101s&fromPage=plp&_requestid=1357077
Total ERK1/2	Cell Signaling Technology	4695S	1:1000	https://www.cellsignal.com/products/primary-antibodies/p44-42-mapk-erk1-2-137f5-

				rabbit-mab/4695?site-search-type=Products&N=4294956287&Ntt=4695s&fromPage=plp&_requestid=1357131
p21	Cell Signaling Technology	2947	1:1000	https://www.cellsignal.com/products/primary-antibodies/p21-waf1-cip1-12d1-rabbit-mab/2947
CD47	Novus Biologicals, LLC	NBP2-31106	1:500	https://www.novusbio.com/products/cd47-antibody-b6h122_nbp2-31106
CD47	Abcam	ab175388	1:500	https://www.abcam.com/products/primary-antibodies/cd47-antibody-ab175388.html
VEGFR3	Santa Cruz Biotechnology	sc-321	1:500	https://www.scbt.com/p/flt-4-antibody-c-20
Epsin 1	Santa Cruz Biotechnology	sc-55556	1:500	https://www.scbt.com/p/epsin-1-antibody-c-11?requestFrom=search
p53	Santa Cruz Biotechnology	sc-126	1:1000	https://www.scbt.com/p/p53-antibody-do-1?requestFrom=search
GAPDH	Santa Cruz Biotechnology	sc-365062	1:2000	https://www.scbt.com/p/gapdh-antibody-g-9?requestFrom=search
TSP1	Proteintech	18304-1-AP	1:400 (1:80 IHC)	https://www.ptglab.com/products/TSP1-Antibody-18304-1-AP.htm
Vinculin 1	Sigma-Aldrich	V4505	1:1000	https://www.sigmaaldrich.com/US/en/product/sigma/v4505
IRDye-conjugated secondary antibodies	Li-Cor Biosciences	925-68070 925-32211 926-32210 926-68071	1:10000	https://www.licor.com/bio/reagents/irdye-secondary-antibodies
SMA	Abcam	ab7817	1:100	https://www.abcam.com/products/primary-antibodies/alpha-smooth-muscle-actin-antibody-1a4-ab7817.html
CD68	Thermo Fisher Scientific	MA5-13324	1:100	https://www.thermofisher.com/antibody/product/CD68-Antibody-clone-KP1-Monoclonal/MA5-13324
LYVE-1	Abcam	ab14917	1:100	https://www.abcam.com/products/primary-antibodies/lyve1-antibody-bsa-and-azide-free-ab14917.html
CD11c	Thermo Fisher Scientific	53-0114-80	1:80	https://www.thermofisher.com/antibody/product/CD11c-Antibody-clone-N418-Monoclonal/53-0114-82
CD3e	Thermo Fisher Scientific	53-0031-80	1:80	https://www.thermofisher.com/antibody/product/CD3e-Antibody-clone-145-2C11-Monoclonal/53-0031-82
CD45	Cell Signaling Technology	70257S	1:70	https://www.cellsignal.com/products/primary-antibodies/cd45-d3f8q-rabbit-mab/70257?site-search-

				type=Products&N=4294956287&Ntt=70257s+&fromPage=plp&_requestid=1362172
CD34	Abcam	ab81289	1:70	https://www.abcam.com/products/primary-antibodies/cd34-antibody-ep373y-ab81289.html
iNOS	Abcam	ab3523	1:100	https://www.abcam.com/products/primary-antibodies/inos-antibody-ab3523.html
Arg1	Sigma-Aldrich	AV45673	1:100	https://www.sigmaaldrich.com/US/en/product/sigma/av45673
Podoplanin	R & D Systems	AF3244	1:40	https://www.rndsystems.com/products/mouse-podoplanin-antibody_af3244
CD31	Abcam	ab28364	1:70	https://www.abcam.com/products/primary-antibodies/cd31-antibody-ab28364.html
Ki67	Cell Signaling Technology	9129	1:100	https://www.cellsignal.com/products/primary-antibodies/ki-67-d3b5-rabbit-mab/9129
IgG control antibody	BioXcell	BE0083	100 µg/mL	https://bioxcell.com/invivomab-mouse-igg1-isotype-control-unknown-specificity-be0083
CD47 blocking antibody	BioXcell	BE0283	100 µg/mL	https://bioxcell.com/invivomab-anti-mouse-human-rat-cd47-iap-be0283

Cultured Cells

Name	**Vendor/ Source**	**Cat #**	**Persistent ID/URL**
Human Dermal Lymphatic Endothelial Cells	PromoCell	C-12217	https://promocell.com/product/human-dermal-lymphatic-endothelial-cells-hdlec/
Human aortic endothelial cells	PromoCell	C-12271	https://promocell.com/product/human-aortic-endothelial-cells-haoec/

Others

Name	**Vendor/ Source**	**Cat #**	**Persistent ID/URL**
Western diet	Envigo	TD.88137	https://insights.envigo.com/hubfs/resources/data-sheets/88137.pdf
Blood glucose monitor	ReliOn		https://www.walmart.com/ip/ReliOn-PRIME-Blood-Glucose-Monitoring-System-Red/20752267
4% paraformaldehyde	Thermo Fisher Scientific	J19943.K2	https://www.thermofisher.com/order/catalog/product/J19943.K2
Optimum cutting temperature compound	Fisher Healthcare	23-730-571	https://www.fishersci.com/shop/products/tissue-plus-o-c-t-compound/23730571
Amplex Red cholesterol assay	Molecular Probes	A12216	https://www.thermofisher.com/order/catalog/product/A12216?SID=srch-srp-A12216
pAAV-*PCSK9*-hD374Y	Vigene Biosciences	NA	NA
Plasma triglyceride kit	Wako Chemicals	992-02892	https://us.vwr.com/store/product/18367215/l-type-triglyceride-m-assay-wako

		998-02992 464-01601	
Oil Red O	Sigma-Aldrich	O0625	https://www.sigmaaldrich.com/US/en/product/sial/o0625
Endothelial cell growth medium	PromoCell	C-22121	https://promocell.com/product/endothelial-cell-growth-medium-mv-2/
Human *CD47* siRNA	Horizon Discovery	M-019505-01-0005	https://horizondiscovery.com/en/gene-modulation/knockdown/sirna/products/sigenome-sirna-reagents?nodeid=entrezgene-961&catalognumber=M-019505-01-0005
Control siRNA	Horizon Discovery	D-001210-01-05	https://horizondiscovery.com/en/gene-modulation/knockdown/controls/products/sigenome-non-targeting-control-sirnas?catalognumber=D-001210-01-05
TransIT-TKO transfection reagent	Mirus Bio LLC	MIR 2155	https://www.mirusbio.com/products/transfection/transit-tko-transfection-reagent#product:MIR%202155
Nitrocellulose membranes	Li-Cor Biosciences	926-31092	https://www.licor.com/bio/reagents/odyssey-nitrocellulose-membranes
Fluoromount-G Mounting Medium, with DAPI	Thermo Fisher Scientific	00-4959-52	https://www.thermofisher.com/order/catalog/product/00-4959-52
Hematoxylin	Fisher Healthcare	22-220-100	https://www.fishersci.com/shop/products/fisher-healthcare-pinnacle-portfolio-hematoxylin-stain-1/22220100
Eosin	Fisher Healthcare	22-220-104	https://www.fishersci.com/shop/products/fisher-healthcare-pinnacle-portfolio-eosin-y-stain/22220104#?keyword=22-220-104
Epredia UltraVision LP HRP polymer and DAB Detection System	Richard Allan Scientific	TL015HD	https://www.fishersci.com/shop/products/ultravision-lp-hrp-polymer-dab-detection-system/TL015HD
Cell Proliferation Reagent WST-1	Roche Diagnostics	5015944001	https://www.sigmaaldrich.com/US/en/product/roche/cellproro
Human recombinant TSP1	Sigma-Aldrich	ECM002	https://www.sigmaaldrich.com/US/en/product/sigma/ecm002
Human recombinant VEGF-C	Peprotech	100-20CD	https://www.peprotech.com/en/recombinant-human-vegf-c-2
FxCycle™ PI/RNase Staining Solution	Thermo Fisher Scientific	F10797	https://www.thermofisher.com/order/catalog/product/F10797
IBI Tri-Isolate RNA Pure Kit	IBI Scientific	IB47632	https://www.ibisci.com/products/tri-isolate-rna-pure-kit?variant=31245650526319
Fast SYBR™ Green Master Mix	Applied Biosystems	4385612	https://www.thermofisher.com/order/catalog/product/4385612

2′,7′-Dichlorofluorescin diacetate	Sigma-Aldrich	D6883	https://www.sigmaaldrich.com/US/en/product/sigma/d6883
DAF-FM diacetate solution	Thermo Fisher Scientific	D23844	https://www.thermofisher.com/order/catalog/product/D23844#:~:text=Invitrogen%E2%84%A2-,DAF%2DFM%20Diacetate%20(4%2DAmino%2D5%2DMethylamino,'%2C7'%2DDifluorofluorescein%20Diacetate)&text=DAF%2DFM%20is%20a%20reagent,to%20form%20a%20fluorescent%20benzotriazole.
LEGENDplex™ bead-based immunoassay	BioLegend	740150	https://www.biolegend.com/en-us/products/legendplex-mouse-inflammation-panel-13-plex-with-filter-plate-10703

ARRIVE GUIDELINES

The ARRIVE guidelines (https://arriveguidelines.org/) are a checklist of recommendations to improve the reporting of research involving animals. Key elements of the study design should be included below to better enable readers to scrutinize the research adequately, evaluate its methodological rigor, and reproduce the methods or findings.

Study Design:

Groups	**Sex**	**Age**	**Number (prior to experiment)**	**Number (after termination)**	**Littermates (Yes/No)**	**Other description**
Cd47^{WT}	Male	8-10 weeks	14	14	Yes	
Cd47$^{\Delta LEC}$	Male	8-10 weeks	13	13	Yes	
Wild-type (VEGF-C Matrigel Plug)	Male	8-10 weeks	7	7	No	
Wild-type (VEGF-C+TSP1+IgG Matrigel Plug)	Male	8-10 weeks	5	5	No	
Wild-type (VEGF-C+TSP1+ CD47-Ab Matrigel Plug)	Male	8-10 weeks	7	7	No	

Sample Size: Based on the previous atherosclerosis animal research work by us and others, we calculated that sufficient sample sizes to detect a true experimental difference with a significance level of 0.05.

Inclusion Criteria: All mice with appropriate genotypes and age were included in the experiments.

Exclusion Criteria: None.

Randomization: Eight- to ten-week-old male C57BL/6J mice were randomly divided into three groups (5-7 mice/group) for the Matrigel plug assay.

Blinding: All *in vivo* data analysis were performed by a blinded investigator.

1. Singla B, Lin HP, Ahn W, White J, Csanyi G. Oxidatively Modified LDL Suppresses Lymphangiogenesis via CD36 Signaling. *Antioxidants (Basel)*. 2021;10. doi: 10.3390/antiox10020331
2. Singla B, Lin HP, Chen A, Ahn W, Ghoshal P, Cherian-Shaw M, White J, Stansfield BK, Csanyi G. Role of R-spondin 2 in arterial lymphangiogenesis and atherosclerosis. *Cardiovasc Res*. 2020. doi: 10.1093/cvr/cvaa244

Figure 1A

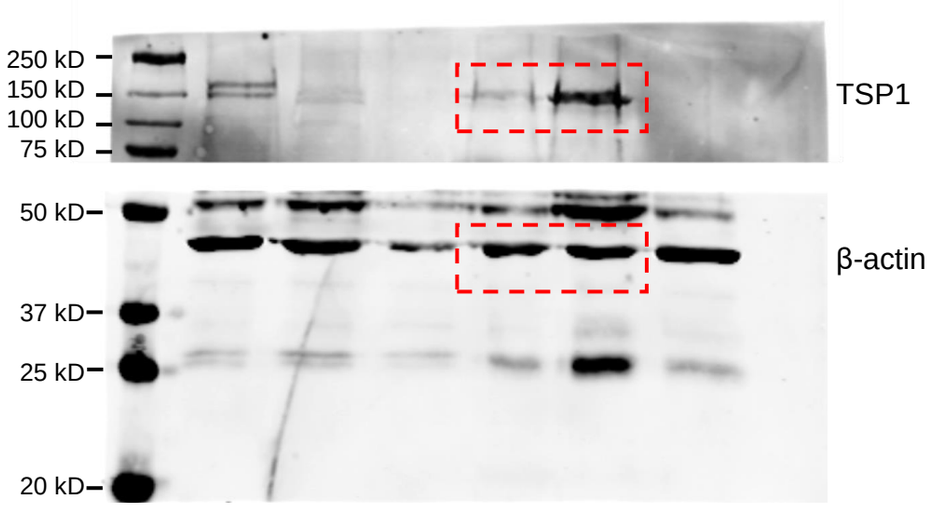

Figure 4A

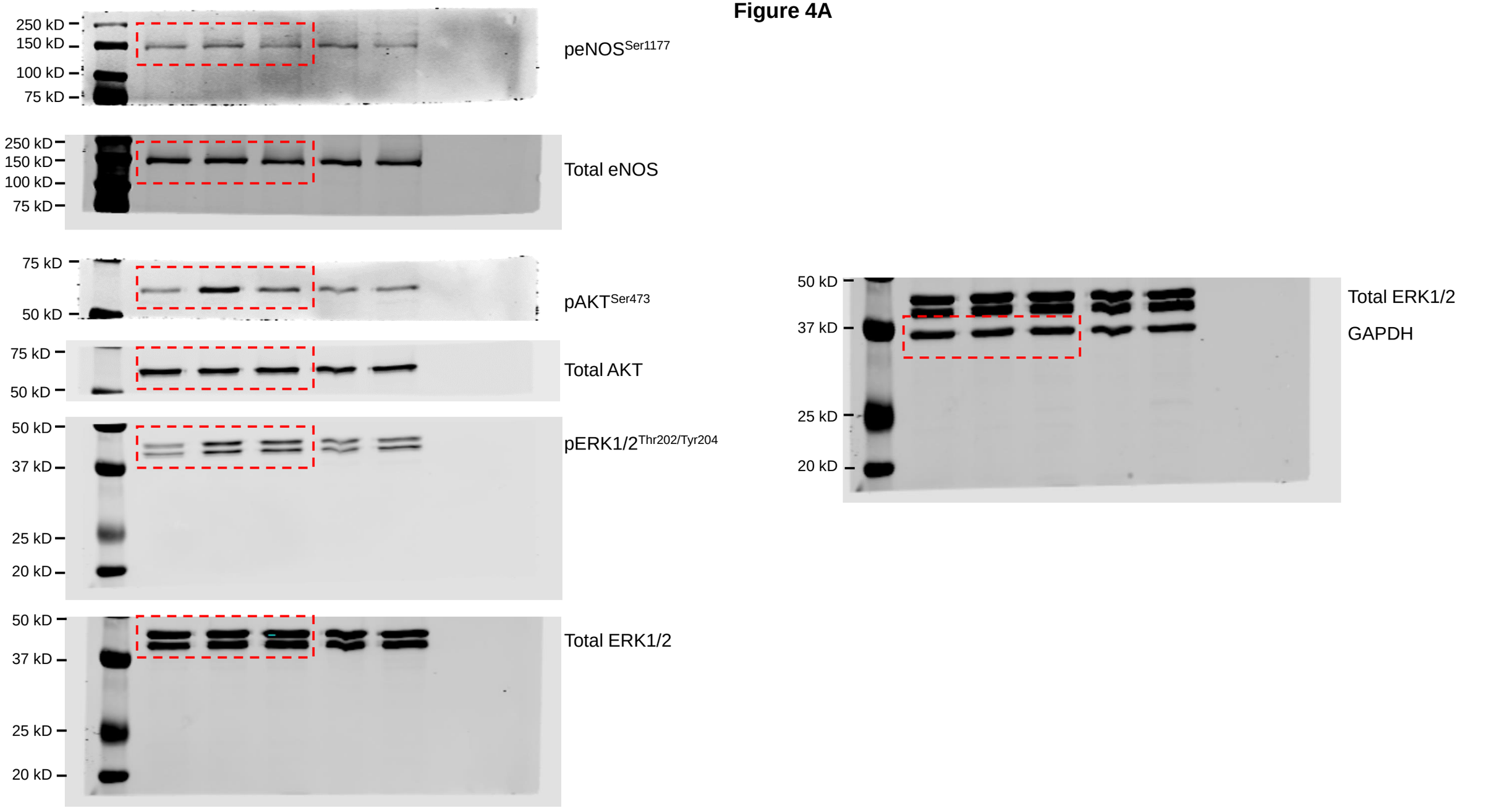
250 kD
150 kD
100 kD
75 kD
peNOS Ser1177
250 kD
150 kD
100 kD
75 kD
Total eNOS
75 kD
50 kD
pAKT Ser473
75 kD
50 kD
Total AKT
50 kD
37 kD
25 kD
20 kD
pERK1/2 Thr202/Tyr204
50 kD
37 kD
25 kD
20 kD
Total ERK1/2
50 kD
37 kD
25 kD
20 kD
Total ERK1/2
GAPDH

Figure 4E

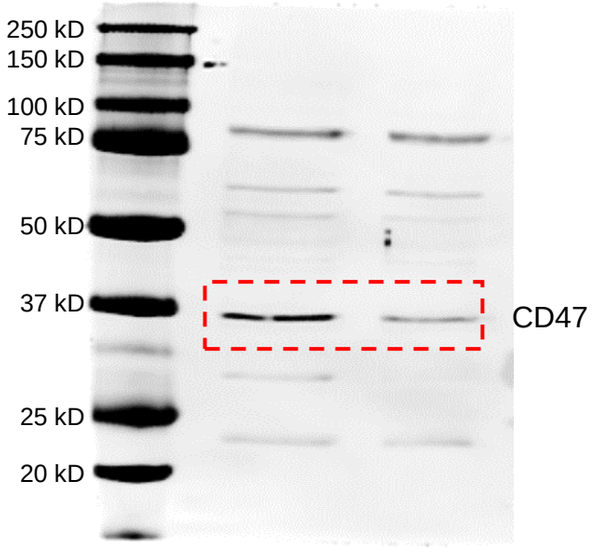
250 kD
150 kD
100 kD
75 kD
50 kD
37 kD
25 kD
20 kD
CD47

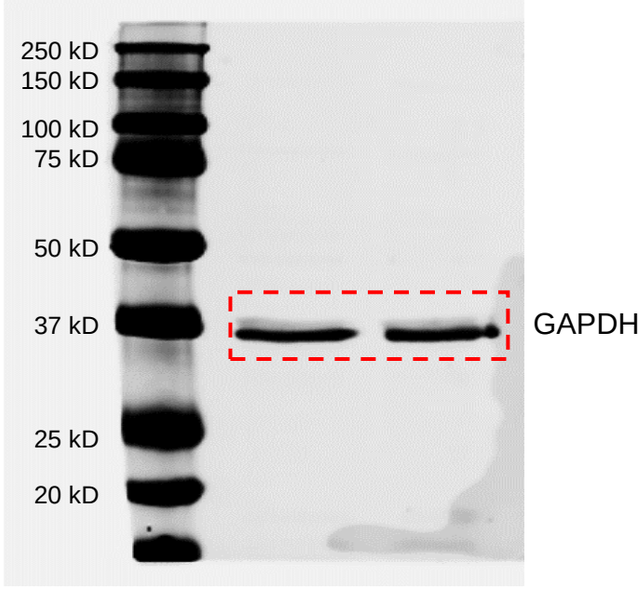
250 kD
150 kD
100 kD
75 kD
50 kD
37 kD
25 kD
20 kD
GAPDH

Figure 4F

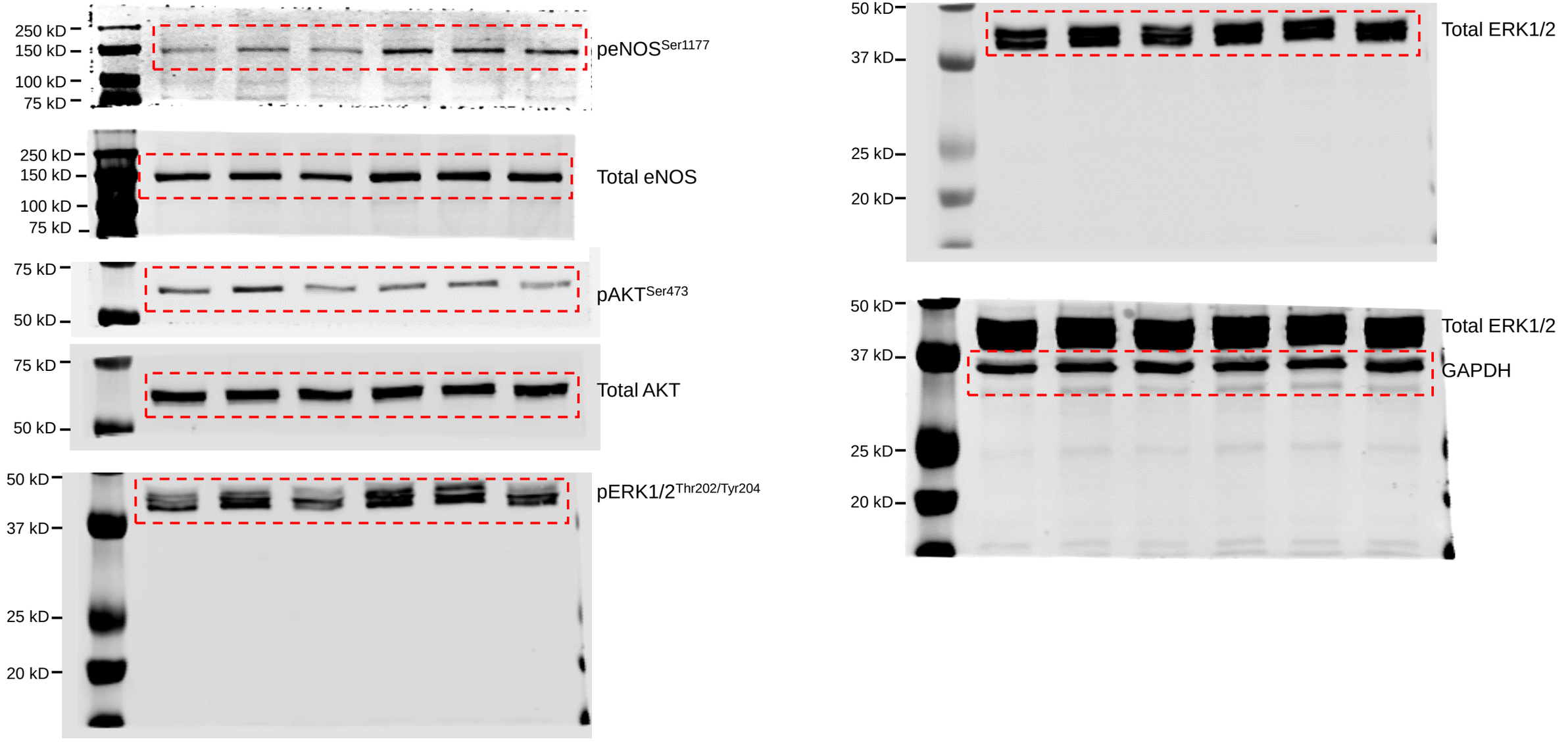
250 kD
150 kD
100 kD
75 kD
peNOS Ser1177
250 kD
150 kD
100 kD
75 kD
Total eNOS
75 kD
50 kD
pAKT Ser473
75 kD
50 kD
Total AKT
50 kD
37 kD
25 kD
20 kD
pERK1/2 Thr202/Tyr204
50 kD
37 kD
25 kD
20 kD
Total ERK1/2
50 kD
37 kD
25 kD
20 kD
Total ERK1/2
GAPDH

Figure S3

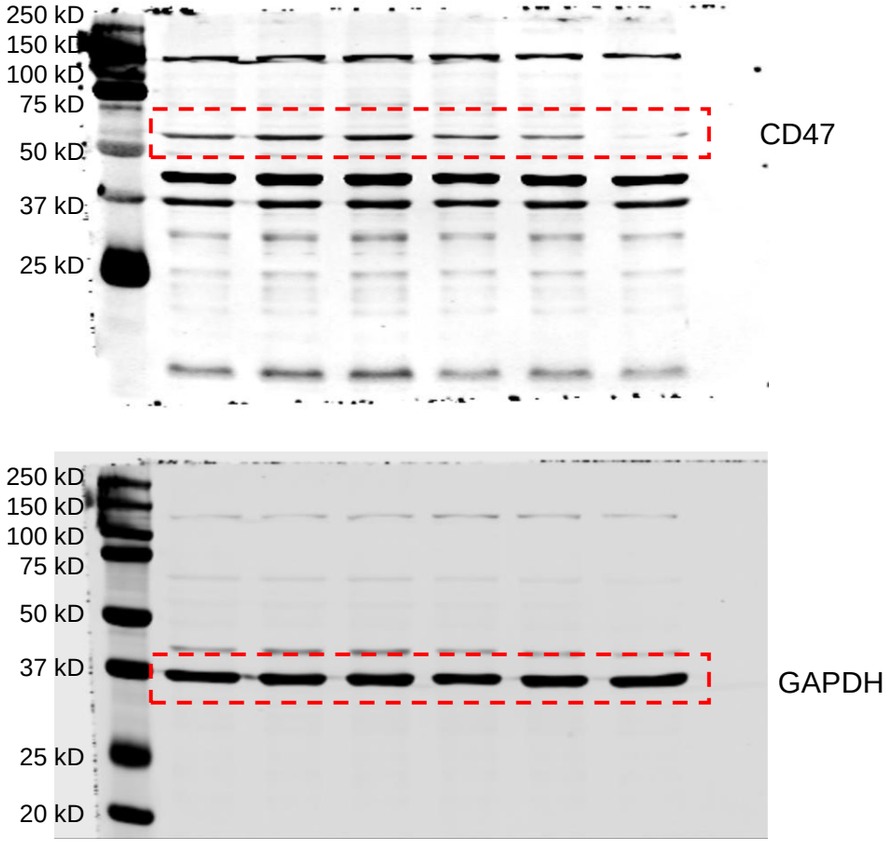
250 kD
150 kD
100 kD
75 kD
50 kD
37 kD
25 kD
CD47
250 kD
150 kD
100 kD
75 kD
50 kD
37 kD
25 kD
20 kD
GAPDH

Figure S5

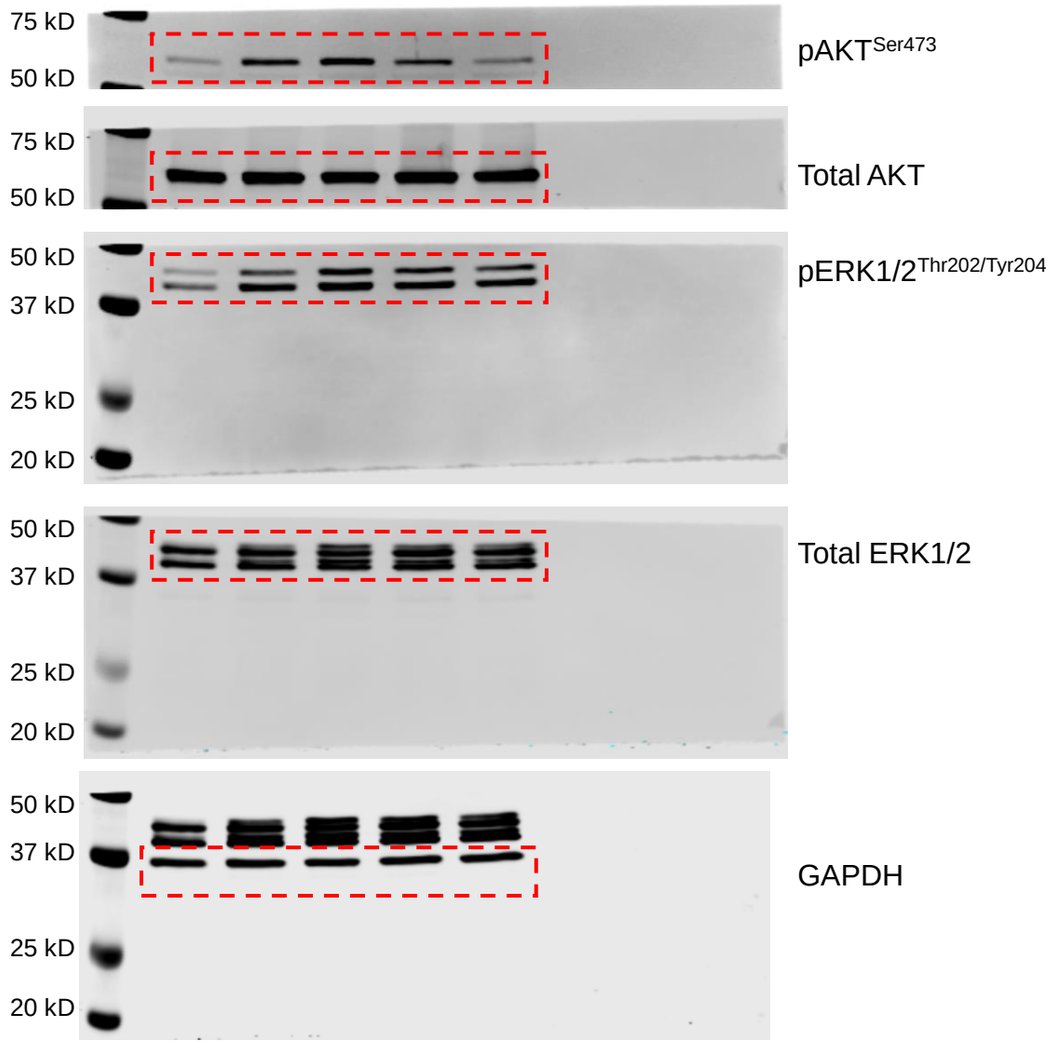
75 kD
50 kD
pAKT Ser473
75 kD
50 kD
Total AKT
50 kD
37 kD
25 kD
20 kD
pERK1/2 Thr202/Tyr204
50 kD
37 kD
25 kD
20 kD
Total ERK1/2
50 kD
37 kD
25 kD
20 kD
GAPDH

Figure S6C

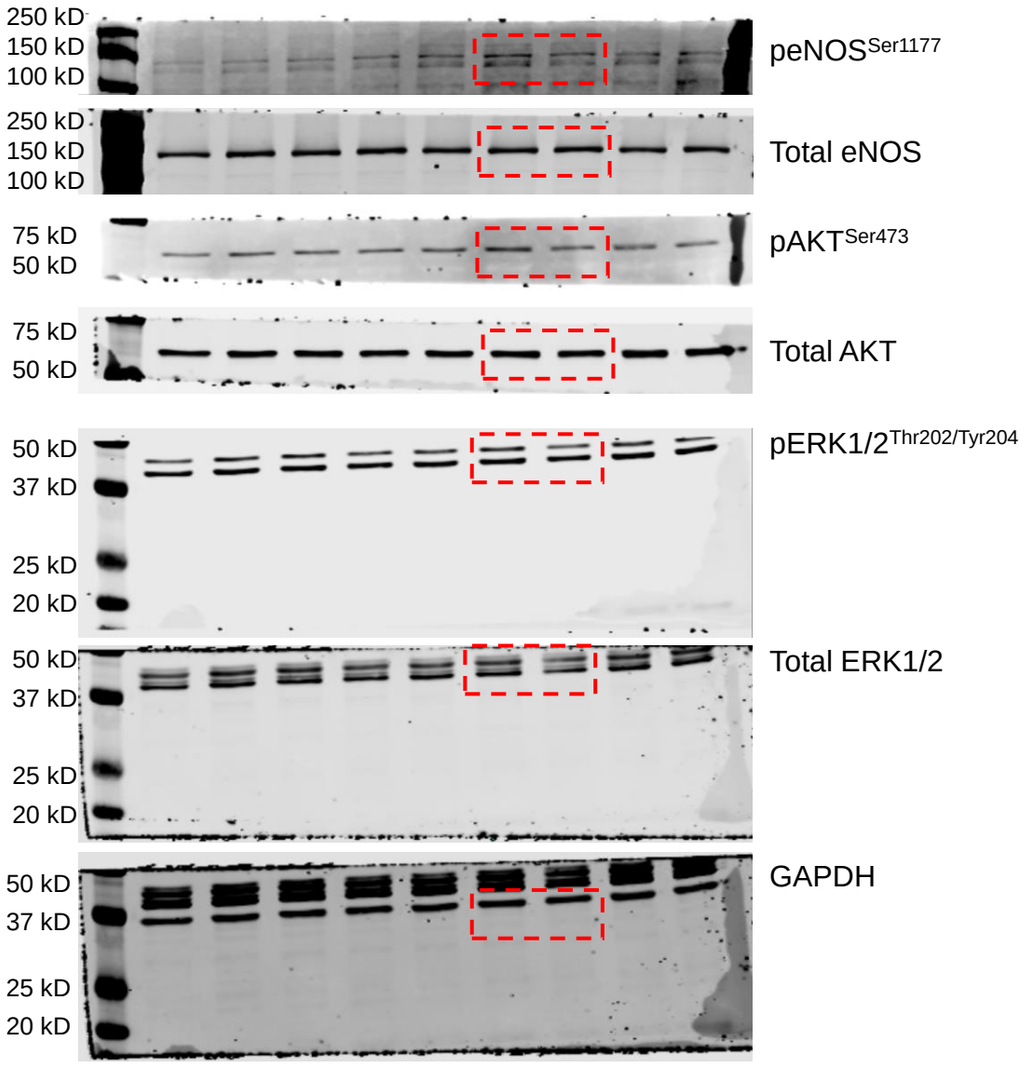
250 kD
150 kD
100 kD
peNOS Ser1177
250 kD
150 kD
100 kD
Total eNOS
75 kD
50 kD
pAKT Ser473
75 kD
50 kD
Total AKT
50 kD
37 kD
25 kD
20 kD
pERK1/2 Thr202/Tyr204
50 kD
37 kD
25 kD
20 kD
Total ERK1/2
50 kD
37 kD
25 kD
20 kD
GAPDH

Figure S7

Figure S7A

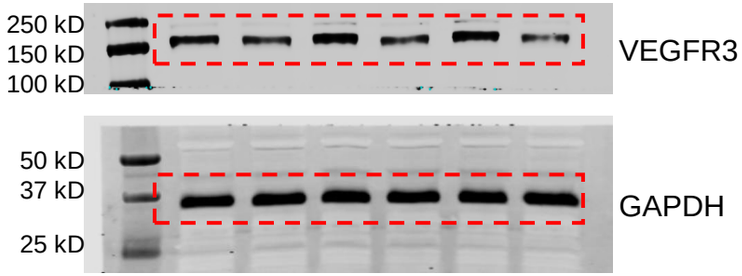

Figure S7C

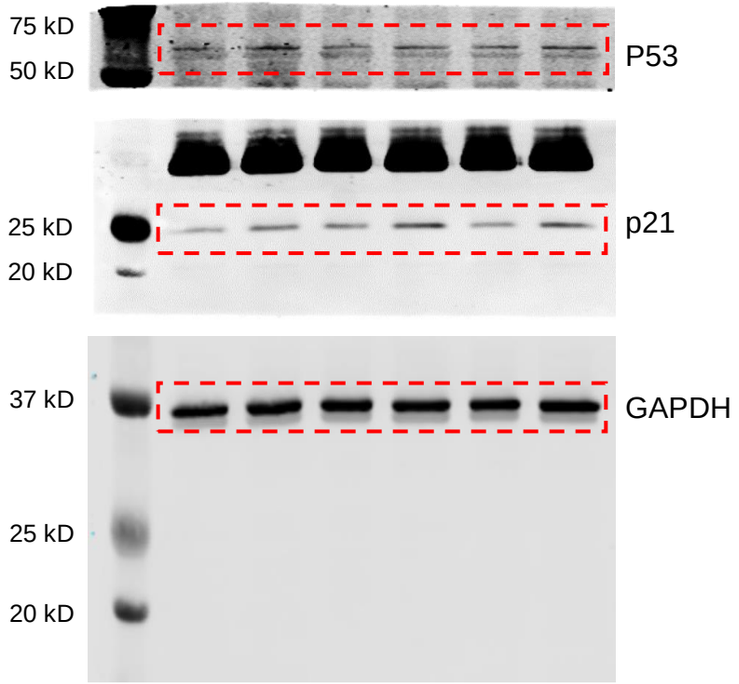

Figure S7D

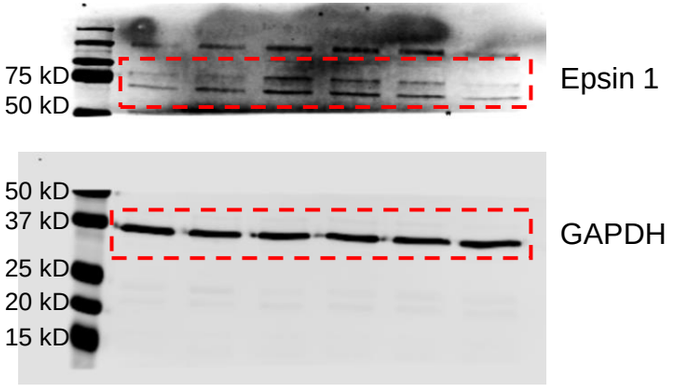

Figure S8

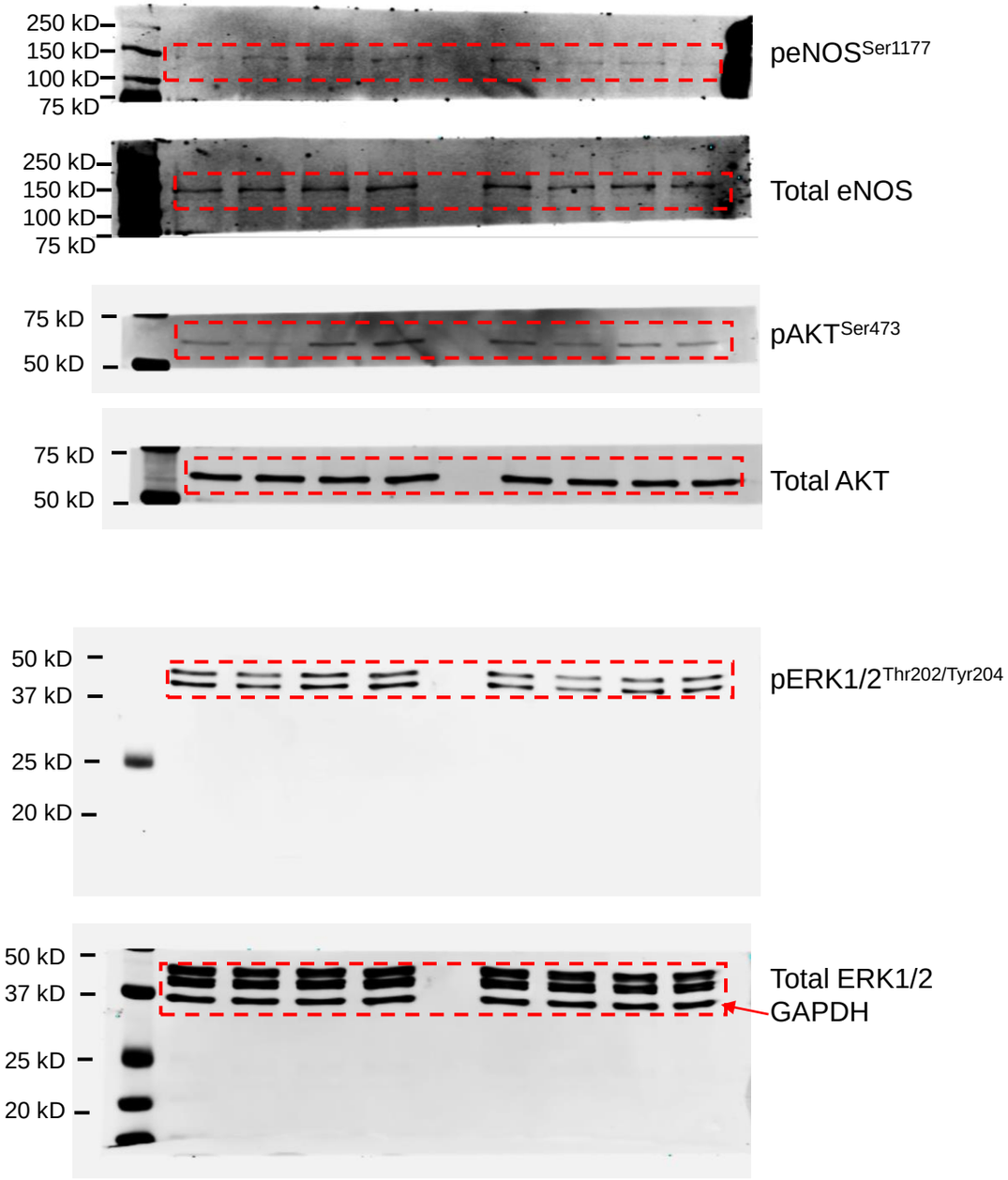
250 kD
150 kD
100 kD
75 kD
peNOS Ser1177
250 kD
150 kD
100 kD
75 kD
Total eNOS
75 kD
50 kD
pAKT Ser473
75 kD
50 kD
Total AKT
50 kD
37 kD
25 kD
20 kD
pERK1/2 Thr202/Tyr204
50 kD
37 kD
25 kD
20 kD
Total ERK1/2
GAPDH